Evaluating a Moist Isentropic Framework for Poleward Moisture Transport: Implications for Water Isotopes over Antarctica

Adriana Bailey[1], Hansi K.A. Singh[2,3], Jesse Nusbaumer [4,5]

[1]National Center for Atmospheric Research, Boulder, CO, USA
[2]Pacific Northwest National Laboratory, US DOE Office of Science, Richland, WA, USA
[3]School of Earth and Ocean Sciences, University of Victoria, Victoria, BC, Canada
[4]NASA Goddard Institute for Space Studies, New York, NY, USA
[5]Center for Climate Systems Research, Columbia University, New York, NY USA

Key Points:

- Model experiments with water tags and isotopic tracers reveal poleward moisture transport largely follows surfaces of constant moist entropy
- Consequently, high-elevation Antarctic sites receive moisture from more equatorward sources than lower elevation sites
- The moist isentropic framework suggests shifts in moisture source regions are tightly linked to changes in temperature and rainout

Corresponding author: Adriana Bailey, abailey@ucar.edu

Abstract

The ability to identify moisture source regions and sinks, and to model the transport pathways that link them in simple yet physical ways, is critical for understanding climate today and in the past. Using water tagging and isotopic tracer experiments in the Community Earth System Model, this work shows that poleward moisture transport largely follows surfaces of constant moist entropy. The analysis not only provides insight into why distinct zonal bands supply moisture to high- and low-elevation polar sites but also explains why changes in these source regions are inherently linked to changes in temperature and rainout. Moreover, because the geometry, and specifically length, of the moist isentropic surfaces describes how much integrated rainout occurs, the analysis provides a physical framework for interpreting the isotopic composition of water in poleward-moving air, thus indicating how variations in moisture transport might influence Antarctic ice cores.

1 Introduction

Moisture transport by the atmospheric circulation critically regulates patterns of temperature, humidity, and precipitation. Describing this transport in simple yet physical ways can provide invaluable insight into how and why these variables change in response to climate forcing. One framework of potential appeal for evaluating outstanding questions about poleward moisture transport is a moist isentropic representation of Earth's atmospheric flow (Pauluis, Czaja, & Korty, 2008, 2010). In this framework, the atmospheric circulation is averaged on surfaces of constant moist entropy instead of a more customary vertical coordinate like pressure.

Pauluis et al. (2010) espoused this choice, arguing that a moist isentropic representation can describe the trajectories of air masses with greater fidelity if the eddies responsible for transport are largely moist adiabatic. This is approximately the case in the extratropics, where much of the poleward moisture transport is accomplished through fast-moving episodic pulses (Fajber, Kushner, & Laliberté, 2018; Laliberté & Kushner, 2014; Messori & Czaja, 2013; Newman, Kiladis, Weickmann, Ralph, & Sardeshmukh, 2012; Sinclair & Dacre, 2019). As a result, moist transport occurs on timescales faster than energy dissipation. This makes it reasonable to assume that extratropical air masses conserve energy (in the form of moist entropy) as they move poleward, even though net poleward heat transport is ultimately driven by radiative imbalances between the equator and the poles. Ostensibly, one could thus use moist isentropic surfaces to define poleward moisture transport pathways and to diagnose and predict variations in moisture source regions.

Examining the accuracy of this framework is of particular interest over Antarctica, where long-standing questions about moisture source regions and sinks, and the transport pathways that link them, affect our understanding of climate today and in the past. Indeed, Lagrangian analyses of air mass trajectories (Sodemann & Stohl, 2009) and water-tagging experiments in general circulation models (GCMs; Noone & Simmonds, 2002) suggest that distinct moisture source regions supply Antarctica's low- and high-elevation sites. Consequently, there is wide geographic variation in correlations between temperature and the isotope ratios of hydrogen and oxygen in Antarctic precipitation (Goursaud, Masson-Delmotte, Favier, Orsi, & Werner, 2018; Kavanaugh & Cuffey, 2003; Masson-Delmotte et al., 2008; Sime, Wolff, Oliver, & Tindall, 2009; Yetang Wang & Jouzel, 2009)—which have traditionally informed our interpretation of past climate from ice cores. Isotopic inversion methods used to reconstruct past climate have tried to address this problem by applying a correction to the isotope-temperature relationship based on estimated conditions for the presumed evaporative source region (e.g. B. Markle, 2017; Stenni et al., 2004, 2010; Uemura et al., 2012; Vimeux, Cuffey, & Jouzel, 2002). If the average poleward moisture flow approximately conserves moist entropy, a moist isentropic framework could offer a valuable conceptual model for explaining how water isotope ratios change with simultaneous variations in moisture source region and temperature, thus bolstering our understanding of the global circulation and its ties to climate.

Here, we evaluate the utility of the moist isentropic framework for describing Antarctic moisture transport in two steps. First, we compare the source regions and transport pathways explicitly identified by water tags in GCM simulations with those indicated by moist isentropes. Second, we compare simulations of isotopic tracers in water vapor from the GCM with theoretical predictions of isotopic distillation for air mass advection along moist isentropic surfaces. Unlike water tags, simulated isotopic tracers can be compared directly with modern and historical observations.

Though ours is not the first study to relate Antarctic moisture transport and isotopic distillation to entropy, previous efforts have considered "dry" isentropic surfaces alone (cf. Noone, 2008). The moist isentropic framework distinguishes itself in at least two ways. First, it accounts for a much larger proportion of mass transport in the extratropics, since much of the moist poleward flow in dry isentropic coordinates is masked by dry equatorward transport at low altitudes (Pauluis et al., 2008, 2010). Second, by accounting for variations in both temperature and humidity, moist isentropes describe the integrated rainout along moisture transport pathways more directly. Since this integrated condensation history determines the isotope ratios of water vapor and precipitation over Antarctica (Dansgaard, 1964), the moist isentropic framework has greater potential to describe how variations in moisture transport influence isotopic records preserved in ice cores.

2 Experimental Design

Following previous investigations (Pauluis et al., 2008, 2010; Sherwood, Roca, Weckwerth, & Andronova, 2010), this study uses equivalent potential temperature (θ_e) as a measure of moist entropy. θ_e is calculated using the approximation of Stull (1988):

$$\theta_e \approx \left(T + \frac{L_v}{c_{pd}} r\right) \left(\frac{p_0}{p}\right)^{R_d/c_{pd}}, \tag{1}$$

in which θ_e varies principally as a function of temperature (T), water vapor mixing ratio (r), and pressure (p). Though the latent heat of vaporization (L_v) and the heat capacity of dry air at constant pressure (c_{pd}) also depend on T, because the dependence is weak over much of the troposphere, we choose to treat these as constant and assign them values of 2.5 $\times 10^6$ J/kg and 1006 J/kg/K, respectively. R_d is the specific gas constant for dry air (287 J/kg/K), and the reference pressure (p_0) is set to 1000 hPa. Estimates of θ_e derived using the approximation suggested by Bryan (2008) were also considered, but do not alter the study's conclusions (Supporting Information). For all estimates of θ_e, we use climatological values of T, p, and r. The input variables are derived from monthly mean output from NCAR's Community Earth System Model (CESM), interpolated to a regular vertical pressure grid that assigns missing values, where necessary, to account for surface topography.

To evaluate the utility of a moist isentropic framework for characterizing the source regions that supply moisture to Antarctica and for delineating the transport pathways by which this moisture moves poleward, two experiments are conducted. In the first experiment, moisture transport pathways mapped by water tracers are compared to surfaces of constant θ_e. Numerical water tracers are implemented in version 5 of the NCAR Community Atmosphere Model (CAM5; Neale et al., 2012) for this purpose. Atmospheric water is tagged with its region of origin (within 10° latitude bands over the oceans), and this tag remains through advection, phase changes, and precipitation (Singh, Bitz, Nusbaumer, & Noone, 2016). CAM5 with water tracers is run within the fully-coupled Community Earth System Model (CESM1; Hurrell et al., 2013) in a 30-yr pre-industrial simulation (i.e. all greenhouse gases, ozone, volcanic constituents, and solar insolation are held at pre-industrial levels), from which seasonal and annual mean climatologies are constructed. All model components are at (nominally) 1° spatial resolution, and the ocean and sea ice are fully dynamic.

In the second experiment, we leverage the fact that, from a Lagrangian frame of reference, the isotope ratios of oxygen and hydrogen in water vapor trace the rainout of air masses, so long as air mass mixing is negligible (e.g. Noone, 2012; Worden, Noone, Bowman, the Tropospheric Emission Spectrometer science team, & data contributors, 2007). (Note that air mass mixing must also be negligble for moisture transport to conserve moist entropy). Due to their lower saturation vapor pressures, isotopically heavy water molecules (e.g. $H_2^{18}O$) are preferentially removed from an air mass as condensation and rainout occur. This preferential loss is well described by distillation theory (Dansgaard, 1964). Therefore, if poleward moisture transport approximates moist isentropic advection, the isotope ratios of water vapor along the isentropes should match distillation predictions.

To evaluate this hypothesis, we define five moist isentropic surfaces using output from CESM. The surfaces (corresponding to θ_e values of 270, 280, 290, 300, and 310 K) are derived by averaging across all meridians south of 25° S that share the same climatological θ_e target value (+/-5 K) at a given pressure level. These target values were selected to approximate 10° spacing over the Southern Hemisphere extratropics; however, the results are not sensitive to the number or spacing of the moist isentropes (Supporting Information). We then compare isotopic distillation expected for a hypothetical air mass advecting along these surfaces to the seasonally averaged oxygen isotope ratios derived from GCM simulations. The simulations come from an isotope-enabled version of CAM5 coupled to an isotope-enabled version of the Community Land Model (CLM4) run with prescribed sea surface temperatures, sea ice, greenhouse gases and aerosols for the years 2000-2014. Details about the model simulation and the underlying isotopic physics can be found in Nusbaumer, Wong, Bardeen, and Noone (2017) and Wong, Nusbaumer, and Noone (2017).

Three variations of distillation are considered in order to estimate uncertainty around the isotopic predictions. For two distillation models we assume that all condensate precipitates immediately, such that the heavy-to-light oxygen isotope ratio ($R={}^{18}O/{}^{16}O$) decreases according to Rayleigh distillation (Dansgaard, 1964; Galewsky, Steen-Larsen, Field, Worden, & Risi, 2016):

$$R = R_0 f^{\alpha-1} \ , \tag{2}$$

where f represents the fraction of water vapor remaining (i.e. r/r_0), α is a temperature-dependent *effective* fractionation factor, and subscript 0 indicates a reference level. We assume the reference level is the pressure level immediately preceding that under consideration along the moist isentropic surface. R is calculated along the surface sequentially, using the climatological values of T and r that define the isentrope and an initial estimate from CESM of the isotope ratio at the lowest pressure level (R_{sfc}). The first distillation model assumes that all water vapor condenses to liquid under saturated conditions, such that α is simply the temperature-dependent *equilibrium* fractionation factor (α_{eq}). In contrast, the second distillation model assumes that all water vapor deposits as ice, such that α must also account for kinetic effects owing to the distinct diffusion rates of heavy and light water under supersaturated conditions (α_{ki}). We use the same α_{eq} formulae reported in Appendix D3 of Bolot, Legras, and Moyer (2013) for the two possible phase changes and estimate α_{ki} following Nusbaumer et al. (2017). A full list of equations may be found in the Supporting Information.

The third distillation model accounts for the fact that the conversion of liquid condensate to precipitation is not customarily 100% efficient (i.e. ϵ=precipitation efficiency<1; see Supporting Information; Bailey, Nusbaumer, & Noone, 2015; Bailey, Toohey, & Noone, 2013; Noone, 2012). The required estimates of condensate concentrations for this modified distillation are derived by summing the climatological mixing ratios of liquid water and ice simulated by CESM along the moist isentropic surfaces. For ϵ, however, we assign a fixed value of 0.5, which closely approximates the precipitation efficiency expected in atmospheric convection (cf. Lutsko & Cronin, 2018) and provides greater isotopic variation from the simple Rayleigh model described above. We do not modify distillation for vapor conversion to ice, as low diffusion rates in ice crystals tend to inhibit isotopic exchange with the surrounding vapor (Bolot et al., 2013; Jouzel & Merlivat, 1984).

As is customary, all isotope ratios are presented relative to Vienna Standard Mean Ocean Water (VSMOW) and reported in units permil:

$$\delta = \left(\frac{R}{R_{VSMOW}} - 1 \right) \times 1000 \; . \tag{3}$$

All isotopic means are mass-weighted.

3 Results

3.1 Water Tracer Experiments

We begin our evaluation of the moist isentropic framework by testing whether it can reliably delineate the moisture source regions and transport pathways to Antarctica identified in water tracer experiments in CESM. Figure 1a shows the relative contributions of distinct Southern Hemisphere oceanic zonal bands to the water vapor concentration at various pressure levels above Antarctica. Figures 1b-g show the normalized, zonal-mean concentrations of atmospheric water vapor evaporated from these source regions, with shading demonstrating that most of the moisture evaporated from each band follows a distinct pathway as it moves poleward. In the extratropics, these moisture plumes approximately align with the moist isentropic surfaces indicated by contours. As a result, zonal bands farthest from Antarctica (i.e., most equatorward) tend to contribute substantially to the upper tropospheric moisture, while higher latitudes contribute moisture to the lower troposphere only (Fig. 1a). This implies that moisture evaporated from the polar ocean (i.e. south of 60° S) is not the same water that reaches Antarctica's high-elevation interior (cf. Noone & Simmonds, 2002; Sodemann & Stohl, 2009). This supposition is confirmed by mapping both the mass-weighted mean latitudes that contribute precipitation to Antarctica (Fig. 2a) and the mean surface moist entropy (Fig. 2b) against the continent's elevation contours.

There are, nevertheless, discrepancies between the extratropical moisture transport pathways identified in the water-tagging experiment and the surfaces of constant moist entropy. In particular, moisture plumes in Figs. 1c-f show an apparent southward shift above approximately 800 hPa, indicating some degree of cross-isentropic mixing. In addition, moisture evaporating from more poleward zonal bands appears more likely to slope down and cross from higher to lower moist isentropes than moisture evaporating from the subtropics. We suspect three factors may be at work.

First, because moist isentropes are not zonally uniform, a perfect match with the zonal water tags is not expected. It is also possible that non-entropy-conserving processes play a role. Moisture recharge by evaporation, for example, will increase the θ_e of air masses that are fully or partially coupled to the ocean surface (i.e. those at relatively low altitudes). Similarly, water loss through precipitation can decrease the θ_e of rising air. However, given the relative insensitivity of θ_e to precipitation (Pauluis et al., 2010), a more likely possibility is that radiative cooling at higher altitudes is sufficient to elicit 'down-gradient' tendencies in poleward-moving air (Yamada & Pauluis, 2016). Previous studies have shown that atmospheric energy transport is well described by diffusion down the meridional moist static energy gradient (e.g. Flannery, 1984; Frierson, Held, & Zurita-Gotor, 2007; Hwang & Frierson, 2010; Roe, Feldl, Armour, Hwang, & Frierson, 2015; Siler, Roe, , & Armour, 2018) and that extratropical potential temperature anomalies move slightly down the moist entropy gradient in the latitude-height plane (Fajber et al., 2018). Examining to what extent net atmospheric heat transport can be deduced from discrepancies between the actual transport pathways and the moist isentropic predictions — particularly in different climate states—would thus be an interesting direction for future research.

3.2 Isotopic tracer experiments

To further evaluate the conceptual accuracy and utility of the moist isentropic framework, we compare June-July-August (JJA) zonal-mean isotope ratios simulated in CESM along five moist isentropic surfaces with water vapor isotope ratios predicted from Rayleigh distillation during air mass advection (Fig. 3). The GCM values fall well within the bounds of the isotopic predictions, given the range of microphysical possibilities represented by the three distillation models considered. Moreover, while there are clear differences among the distillation predictions, due to variations in effective fractionation (α) or the degree of precipitation efficiency (ϵ), the resultant isotopic differences at high latitudes are smaller than those produced when crossing from one moist isentropic surface to the next. In particular, variations in ϵ make little difference except in the driest parts of the atmosphere (Fig. 3c), such as one might find over the highest elevations of the Antarctic continent. However, because low mixing ratios (which make up the isotope ratio denominator) tend to accentuate small isotopic inaccuracies, it is difficult to gauge whether these results confirm the importance of microphysical factors in regulating water isotope ratios in extremely cold and dry climates, as others have argued (Schoenemann, Steig, Ding, Markle, & Schauer, 2018). Regardless, for the extratropics as a whole, Fig. 3 shows that the dynamics that set the geometry of the moist isentropic surfaces are the more important constraint on the atmosphere's zonal-mean isotopic composition.

Figure 4 emphasizes the importance of the moist isentrope geometry by showing the seasonal shift in water vapor isotope ratios along the θ_e surfaces. As austral winter (JJA) gives way to summer (December-January-February, DJF), the surfaces are displaced nearly 10° poleward, contracting and shortening as a result. It is this change in surface shape—and specifically length—that matters most for the shift in isotopic composition (tens of permil over Antarctica). Figure 4b illustrates this point by considering the effects of seasonal variations in the individual factors that control distillation along the moist isentropes: namely, the isotopic composition of the moisture source, the effective rainout along the moisture trajectory, and the temperature at which condensation occurs. These factors are represented by R_{sfc}, f, and α_{eq}—the full set of inputs required for Equation 2 under the assumptions of Rayleigh distillation. The broken lines in Fig. 4b indicate the seasonal shift in isotopic composition that occurs when DJF values are substituted for JJA values for any single factor: it is hardly detectable at most locations. What this implies is that it is primarily the length of the surface—controlling how much total rainout and distillation occurs—that influences the seasonal isotopic shift that the GCM produces. This result provides evidence that seasonal isotopic variations are tightly tied to variations in mean moisture length scale and corroborates the work of Feng, Faiia, and Posmentier (2009), who argued that precipitation $\delta^{18}O$ seasonality depends on the zonal position of the subtropical highs and coincident global moisture source regions.

4 Implications

Though mean poleward moisture transport may not be strictly moist isentropic, the results of this study provide evidence that a moist isentropic representation of the meridional flow offers a useful lens for describing moisture transport and for linking changes in transport to changes in climate. First, moist entropy provides a concise argument for why high- and low-elevation Antarctic sites are linked to distinct moisture source regions (Fig. 2; Noone & Simmonds, 2002; Sodemann & Stohl, 2009) and exhibit different isotope-temperature scaling relationships geographically and temporally (Goursaud et al., 2018; Kavanaugh & Cuffey, 2003; Masson-Delmotte et al., 2008; Sime et al., 2009; Yetang Wang & Jouzel, 2009). Low-altitude polar air masses simply cannot gain enough potential energy (through loss of latent and sensible heat) to reach the high-elevation continental interior while still conserving moist entropy. The moist isentropic framework thus reinforces the findings of earlier studies by Noone and Simmonds (2002) and Noone (2008), which argued that low buoyancy and potential temperature limit the influence of evaporation from Antarctica's coastal waters on the moisture budget—and hence isotopic records—of ice core drilling sites on the Antarctic plateau.

Observed isotope ratios of water vapor and precipitation from near the summit of Dome C (3233 m, Casado et al., 2016; Goursaud et al., 2018) further support this contention. As shown in Fig. 4a, the observed isotope ratios are simply too low to be consistent with advection of evaporate along the lowest θ_e surfaces. Indeed, the water vapor measurements (collected between December 2014 and January 2015) are most consistent with the 300 K surface, whose affiliated source region migrates between 40° and 45° S annually. The center of this zonal band aligns almost exactly with the mean annual moisture source latitude identified by water tags in CESM (Fig. 2a). Previous studies using other tracer methods have demonstrated similar links between the mid-latitude surface and higher altitudes in the Arctic, indicating that isentropic transport can effectively deliver mid-latitude pollution and warming signals to polar regions (Orbe, Holzer, Polvani, & Waugh, 2013; Orbe et al., 2015).

Second, our results suggest that it is not so much the differences in moisture source per se that cause Antarctica's isotope-temperature relationships to vary with elevation, but rather the differences in total rainout dictated by the distinct θ_e surfaces that link the source regions to these sites (Fig. 4). As clear from Equation 1, both temperature and moisture define the geometry of the atmosphere's moist isentropic surfaces, and these variables themselves are strongly linked to one another through the Clausius-Clayperon relationship, assuming variations in relative humidity are negligible. Consequently, shifts in temperature imply a change in the latitude and pressure coordinates of the moist isentropes. The resultant modification to surface geometry not only affects hydrological linkages between Antarctica and lower-latitude regions, but also influences the mean distance over which moisture is transported. Our study suggests it is this change in mean moisture length scale that alters the total rainout experienced by poleward moving air and, ultimately, its isotopic composition.

Finally, our analysis helps demonstrate the utility of idealized distillation models by elucidating why these models work despite their simplicity. Because mixing is a cross-isentropic process, distillation can provide fairly accurate predictions of isotopic changes if the moisture transport pathways considered mostly conserve moist entropy, as we have shown is the case in the extratropics. Conversely, because moist (as compared to dry) isentropes account for variations in both temperature and precipitable water with altitude, they offer a useful conceptual framework for predicting and interpreting isotopic distillation with poleward transport for a given climate state.

5 Conclusion

Using a single state-of-the-art GCM, this study shows that poleward moisture transport is largely consistent with a moist isentropic view of the mean atmospheric flow. Both numerical water tracer and isotopic tracer experiments in the Community Earth System Model (CESM) demonstrate that moist entropy is a useful framework for identifying the moisture source regions that supply moisture to Antarctica and for delineating the hydrological pathways by which moisture sources and sinks are linked. The fact that our results are self-consistent between the distinct tracer experiments adds a degree of confidence to the results, though further evaluation, using other GCMs and targeted observational campaigns, would be desirable. The isotopic results are particularly valuable in that they can be compared directly to observations, whether remote or in situ (e.g. by aircraft).

The moist isentropic framework provides a simple yet physical explanation for a number of key relationships. It shows, for instance, that high- and low-elevation sites at high-latitudes are connected to distinct moisture source regions, with higher-elevation sites receiving moisture from more equatorward sources, due to the shape of the moist isentropic surfaces. The surface geometry also controls the mean distance moisture travels by altering the integrated rainout experienced by poleward moving air. Since this total rainout regulates isotopic distillation to first order, conservation of moist entropy provides a conceptual basis for understanding how changes in meridional transport influence the isotope ratios of water vapor over Antarctica, as others have intimated (B. R. Markle et al., 2017; Noone, 2008; Stenni et al., 2004, 2010; Vimeux et al., 2002). Moreover, because the isentropic surface geometry is largely defined by atmospheric temperature, moist entropy offers a possible framework for predicting variations in moisture source region and moisture length scale with changes in climate.

Acknowledgments

This material is based upon work supported by the National Center for Atmospheric Research, which is a major facility sponsored by the National Science Foundation under Cooperative Agreement No. 1852977. HKAS is grateful for generous funding through the Linus Pauling Distinguished Postdoctoral Fellowship, sponsored by Pacific Northwest National Laboratory and the US Department of Energy Office of Science. JN was supported by the NASA Post-doctoral Program (NPP) fellowship at NASA GISS, along with NASA grant NNH13ZDA001N-NEWS. The authors thank Cecilia Bitz and David Noone for encouraging us to pursue this line of research, Robert Fajber for useful theoretical discussions, Isla Simpson and Christina McCluskey for their thoughtful feedback on an initial draft of the manuscript, and Bradley Markle and an anonymous reviewer for their excellent suggestions for improving the analysis and its presentation. CESM output data used in this study are available at *https* : //*doi.org*/10.5281/*zenodo*.2595607.

References

Bailey, A., Nusbaumer, J., & Noone, D. (2015). Precipitation efficiency derived from isotope ratios in water vapor distinguishes dynamical and microphysical influences on subtropical atmospheric constituents. *Journal of Geophysical Research: Atmospheres*, *120*(18), 9119–9137. doi: 10.1002/2015JD023403

Bailey, A., Toohey, D., & Noone, D. (2013). Characterizing moisture exchange between the hawaiian convective boundary layer and free troposphere using stable isotopes in water. *Journal of Geophysical Research: Atmospheres*, *118*(15), 8208–8221. doi: 10.1002/jgrd.50639

Bolot, M., Legras, B., & Moyer, E. (2013). Modelling and interpreting the isotopic composition of water vapour in convective updrafts. *Atmospheric Chemistry and Physics*, *13*(16), 7903–7935. doi: 10.5194/acp-13-7903-2013

Bryan, G. H. (2008). On the computation of pseudoadiabatic entropy and equivalent potential temperature. *Monthly Weather Review*, *136*(12), 5239–5245. doi: 10

.1175/2008MWR2593.1

Casado, M., Landais, A., Masson-Delmotte, V., Genthon, C., Kerstel, E., Kassi, S., … Cermak, P. (2016). Continuous measurements of isotopic composition of water vapour on the east antarctic plateau. *Atmospheric Chemistry and Physics*, *16*, 8521–8538. doi: 10.5194/acp-16-8521-20163

Dansgaard, W. (1964). Stable isotopes in precipitation. *Tellus*, *16*(4), 436–468. doi: 10.3402/tellusa.v16i4.8993

Fajber, R., Kushner, P. J., & Laliberté, F. (2018). Influence of midlatitude surface thermal anomalies on the polar midtroposphere in an idealized moist model. *Journal of the Atmospheric Sciences*, *75*(4), 1089–1104. doi: 10.1175/JAS-D-17-0283.1

Feng, X., Faiia, A. M., & Posmentier, E. S. (2009). Seasonality of isotopes in precipitation: A global perspective. *Journal of Geophysical Research: Atmospheres*, *114*, D08116. doi: 10.1029/2008JD011279

Flannery, B. P. (1984). Energy balance models incorporating transport of thermal and latent energy. *Journal of the Atmospheric Sciences*, *41*(3), 414–421. doi: https://doi.org/10.1175/1520-0469(1984)041⟨0414:EBMITO⟩2.0.CO;2

Frierson, D. M. W., Held, I. M., & Zurita-Gotor, P. (2007). A gray-radiation aquaplanet moist gcm. part ii: Energy transport in altered climates. *Journal of the Atmospheric Sciences*, *64*, 1680–1693. doi: 10.1175/JAS3913.1

Galewsky, J., Steen-Larsen, H. C., Field, R. D., Worden, J., & Risi, C. (2016). Stable isotopes in atmospheric water vapor and applications to the hydrologic cycle. *Reviews of Geophysics*, *54*(4), 809-865. doi: 10.1002/2015RG000512

Goursaud, S., Masson-Delmotte, V., Favier, V., Orsi, A., & Werner, M. (2018). Water stable isotope spatio-temporal variability in antarctica in 1960–2013: observations and simulations from the echam5-wiso atmospheric general circulation model. *Climate of the Past*, *14*(6), 923–946. doi: 10.5194/cp-14-923-2018]

Hurrell, J., Holland, M., Gent, P., Ghan, S., Kay, J., Kushner, P., … Marshall, S. (2013). The community earth system model: A framework for collaborative research. *Bulletin of the American Meteorological Society*, *94*, 1339-1360. doi: 10.1175/BAMS-D-12-00121.1

Hwang, Y.-T., & Frierson, D. (2010). Increasing atmospheric poleward energy transport with global warming. *Geophysical Research Letters*, *37*, L24807. doi: 10

.1029/2010GL045440

Jouzel, J., & Merlivat, L. (1984). Deuterium and oxygen 18 in precipitation: Modeling of the isotopic effects during snow formation. *Journal of Geophysical Research: Atmospheres*, *89*(D7), 11749–11757. doi: 10.1029/JD089iD07p11749

Kavanaugh, J. L., & Cuffey, K. M. (2003). Space and time variation of δ^{18}o and δd in antarctic precipitaiton revisited. *Global Biogeochemical Cycles*, *17*, 1017. doi: 10.1029/2002GB001910

Laliberté, F., & Kushner, P. J. (2014). Midlatitude moisture contribution to recent arctic tropospheric summertime variability. *Journal of Climate*, *27*, 5693–5707. doi: 10.1175/JCLI-D-13-00721.1

Lutsko, N. J., & Cronin, T. W. (2018). Increase in precipitation efficiency with surface warming in radiative-convective equilibrium. *Journal of Advances in Modeling Earth Systems*, *10*(11), 2992–3010. doi: 10.1029/2018MS001482

Markle, B. (2017). *Climate dynamics revealed in ice cores: advances in techniques, theory, and interpretation* (Doctoral dissertation, University of Washington). Retrieved from `http://hdl.handle.net/1773/40391`

Markle, B. R., Steig, E. J., Buizert, C., Schoenemann, S. W., Bitz, C. M., Fudge, T. J., ... Sowers, T. (2017). Global atmospheric teleconnections during dansgaard-oeschger events. *Nature Geoscience*.

Masson-Delmotte, V., Hou, S., Ekaykin, A., Jouzel, J., Aristarain, A., Bernardo, R., ... White, J. (2008). A review of antarctic surface snow isotopic composition: Observations, atmospheric circulation, and isotopic modeling. *Journal of Climate*, *21*(13), 3359–3387. doi: 10.1175/2007JCLI2139.1

Messori, G., & Czaja, A. (2013). On the sporadic nature of meridional heat transport by transient eddies. *Quarterly Journal of the Royal Meteorological Society*, *139*, 999–1008. doi: 10.1002/qj.2011

Neale, R., Chen, C.-C., Gettelman, A., Lauritzen, P., Park, S., Williamson, D., ... and, M. T. (2012, Nov). *Description of ncar community atmosphere model (cam 5.0)* (NCAR Technical Note Nos. TN-486+STR). NCAR.

Newman, M., Kiladis, G. N., Weickmann, K. M., Ralph, F. M., & Sardeshmukh, P. D. (2012). Relative contributions of synoptic and low-frequency eddies to time-mean atmospheric moisture transport, including the role of atmospheric rivers. *Journal of Climate*, *25*, 7341–7361. doi: 10.1175/JCLI-D-11-00665.1

Noone, D. (2008). The influence of midlatitude and tropical overturning circulation on the isotopic composition of atmospheric water vapor and antarctic precipitation. *Journal of Geophysical Research: Atmospheres*, *113*, D04102,. doi: 10.1029/2007JD008892

Noone, D. (2012). Pairing measurements of the water vapor isotope ratio with humidity to deduce atmospheric moistening and dehydration in the tropical midtroposphere. *Journal of Climate*, *25*(13), 4476–4494. doi: 10.1175/JCLI-D-11-00582.1

Noone, D., & Simmonds, I. (2002). Annular variations in moisture transport mechanisms and the abundance of δ18o in antarctic snow. *Journal of Geophysical Research: Atmospheres*, *107*(D24), 4742. doi: 10.1029/2002JD002262

Nusbaumer, J., Wong, T. E., Bardeen, C., & Noone, D. (2017). Evaluating hydrological processes in the community atmosphere model version 5 (cam5) using stable isotope ratios of water. *Journal of Advances in Modeling Earth Systems*, *9*(2), 949–977. doi: 10.1002/2016MS000839

Orbe, C., Holzer, M., Polvani, L. M., & Waugh, D. (2013). Air mass origin as a diagnostic of tropospheric transport. *Journal of Geophysical Research: Atmospheres*, *118*, 1459–1470. doi: 10.1002/jgrd.50133

Orbe, C., Newman, P. A., Waugh, D. W., Holzer, M., Oman, L. D., Li, F., & Polvani, L. M. (2015). Airmass origin in the arctic. part i: Seasonality. *Journal of Climate*, *28*, 4997–5014. doi: 10.1175/JCLI-D-14-00720.1

Pauluis, O., Czaja, A., & Korty, R. (2008). The global atmospheric circulation on moist isentropes. *Science*, *321*(5892), 1075–1078. doi: 10.1126/science.1159649

Pauluis, O., Czaja, A., & Korty, R. (2010). The global atmospheric circulation in moist isentropic coordinates. *Journal of Climate*, *23*(11), 3077–3093. doi: 10.1175/2009JCLI2789.1

Roe, G., Feldl, N., Armour, K., Hwang, Y.-T., & Frierson, D. (2015). The remote impacts of climate feedbacks on regional climate predictability. *Nature Geoscience*, *8*, 135-139. doi: 10.1038/NGEO2346

Schoenemann, S. W., Steig, E. J., Ding, Q., Markle, B. R., & Schauer, A. J. (2018). Triple water-isotopologue record from wais divide, antarctica: Controls on glacial-interglacial changes in 17oexcess of precipitation. *Journal of Geophysi-*

cal Research Atmospheres, *119*, 8741–8767. doi: 10.1002/2014JD021770

Sherwood, S., Roca, R., Weckwerth, T., & Andronova, N. (2010). Tropospheric water vapor, convection, and climate. *Reviews of Geophysics*, *48*(2). doi: 10.1029/2009rg000301

Siler, N., Roe, G. H., , & Armour, K. C. (2018). Insights into the zonal-mean response of the hydrologic cycle to global warming from a diffusive energy balance model. *Journal of Climate*, *31*, 7481– 7493. doi: 10.1175/JCLI-D-18-0081.1

Sime, L. C., Wolff, E. W., Oliver, K. I. C., & Tindall, J. C. (2009). Evidence for warmer interglacials in east antarctic ice cores. *Nature*, *462*, 342–346. doi: 10.1038/nature08564

Sinclair, V. A., & Dacre, H. F. (2019). Which extratropical cyclones contribute most to the transport of moisture in the southern hemisphere? *Journal of Geophysical Research: Atmospheres*, *124*, 1–21. doi: 10.1029/2018JD028766

Singh, H., Bitz, C., Nusbaumer, J., & Noone, D. (2016). A mathematical framework for analysis of water tracers: Part 1: Development of theory and application to the preindustrial mean state. *Journal of Advances in Modeling Earth Systems*, *8*(2), 991–1013. doi: 10.1002/2016MS000649

Sodemann, H., & Stohl, A. (2009). Asymmetries in the moisture origin of antarctic precipitation. *Geophysical research letters*, *36*, L22803. doi: 10.1029/2009GL040242

Stenni, B., Jouzel, J., Masson-Delmotte, V., Röthlisberger, R., Castellano, E., Cattani, O., . . . Udisti, R. (2004). A late-glacial high-resolution site and source temperature record derived from the epica dome c isotope records (east antarctica). *Earth and Planetary Science Letters*, *217*, 183–195. doi: 10.1016/S0012-821X(03)00574-0

Stenni, B., Masson-Delmotte, V., Selmo, E., Oerter, H., andR. Röthlisberger, H. M., Jouzel, J., . . . Udisti, R. (2010). Deuterium excess records of epica dome c and dronning maud land ice cores (east antarctica). *Quarternary Science Reviews*, *29*, 146–159. doi: 10.1016/j.quascirev.2009.10.009

Stull, R. B. (1988). *An introduction to boundary layer meteorology* (Vol. 13). Springer Science & Business Media.

Uemura, R., Masson-Delmotte, V., Jouzel, J., Landais, A., Motoyama, H., & Stenni,

B. (2012). Ranges of moisture-source temperature estimated from antarctic ice cores stable isotope records over glacial-interglacial cycles. *Climate of the Past*, *8*, 1109-1125. doi: 10.5194/cp-8-1109-2012

Vimeux, F., Cuffey, K. M., & Jouzel, J. (2002). New insights into southern hemisphere temperature changes from vostok ice cores using deuterium excess correction. *Earth and Planetary Science Letters*, *203*, 829–843. doi: 10.1016/S0012-821X(02)00950-0

Wong, T. E., Nusbaumer, J., & Noone, D. C. (2017). Evaluation of modeled land-atmosphere exchanges with a comprehensive water isotope fractionation scheme in version 4 of the community land model. , *9*(2), 978–1001. doi: 10.1002/2016MS000842

Worden, J., Noone, D., Bowman, K., the Tropospheric Emission Spectrometer science team, & data contributors. (2007). Importance of rain evaporation and terrestrial sources in the tropical water cycle. *Nature*, *445*, 528–532. doi: 10.1038/nature05508

Yamada, R., & Pauluis, O. (2016). Momentum balance and eliassen–palm flux on moist isentropic surfaces. *Journal of the Atmospheric Sciences*, *73*(3), 1293–1314. doi: 10.1175/JAS-D-15-0229.1

Yetang Wang, V. M.-D., Shugui Hou, & Jouzel, J. (2009). A new spatial distribution map of δ^{18}o in antarctic surface snow. *Geophysical Research Letters*, *36*, L06501. doi: 10.1029/2008GL036939

Figure 1. Zonal-mean moisture source regions and pathways for Southern Hemisphere atmospheric water vapor: **(a)** contribution of distinct oceanic zonal bands to the annual mean water vapor over Antarctica, normalized by the water vapor concentration at each pressure level; and **(b-g)** (shading) normalized, annual and zonal mean distributions of water vapor in the Southern Hemisphere sourced from (b) 60° S to the pole, (c) 50° S to 60° S, (d) 40° S to 50° S, (e) 30° S to 40° S, (f) 20° S to 30° S, and (g) 10° S to 20° S, overlaid with (contours) equivalent potential temperature (K). A representative surface pressure for Dome C, Antarctica (3233 m, discussed later in the text) is indicated by the dashed line in (a).

Figure 2. Moisture source latitudes for Antarctic precipitation and moist entropy at the surface: **(a)** annual mean latitude from which precipitation originates (degrees); and **(b)** θ_e at the surface (K). Contours show surface elevation (m) in both panels. The black dot marks the location of Dome C observations (discussed later in the text) in panel (a).

Figure 3. Water vapor isotope ratios on moist isentropic surfaces. **(a)** JJA $\delta^{18}O$ values predicted for five moist isentropic surfaces (distinguished by color and labeled in K) shown as a function of latitude. Predictions come from (dashed line) modified distillation with a precipitation efficiency (ϵ) of 0.5, assuming all water vapor condenses to liquid; (solid line) Rayleigh distillation (ϵ=1.0), assuming all water vapor condenses to liquid; (dotted line) Rayleigh distillation, assuming all water vapor deposits as ice; and (crosses) CESM. **(b)** Predictions from the distillation models identified in (a) are plotted against simulated isotope ratios in water vapor from CESM, with the 1:1 line shown in gray. **(c)** Differences between the various distillation models and CESM are shown as a function of water vapor mixing ratio (g/kg), with the zero-line shown in gray. Note the reversed y-axis in all panels.

Figure 4. Seasonal variations in water vapor isotope ratios along moist isentropic surfaces: **(a)** (thin line) JJA and (thick line) DJF $\delta^{18}O$ values predicted for five moist isentropic surfaces (distinguished by color and labeled in K) shown as a function of latitude. Predictions come from Rayleigh distillation assuming all water vapor condenses to liquid. Symbols show isotope ratios from CESM and observations from Dome C, Antarctica, for comparison. The open circle with vertical bar identifies the mean and total range of $\delta^{18}O$ in water vapor (Dome C_V) observed by Casado et al. (2016) during December 2014-January 2015. The closed circle shows the annual mean precipitation $\delta^{18}O$ (Dome C_P) reported by Goursaud et al. (2018). **(b)** Variations in the $\delta^{18}O$ values along JJA moist isentropic surfaces produced when using DJF values for (dashed line) R_{sfc} (the water vapor isotope ratio near the moisture source), (dotted line) f (one minus the effective rainout along the moisture trajectory), and (dotted-dashed line) α_{eq}, which is determined by atmospheric temperature. Scatterplots of DJF v. JJA values for these three factors are provided in the Supporting Information.

Figure1.

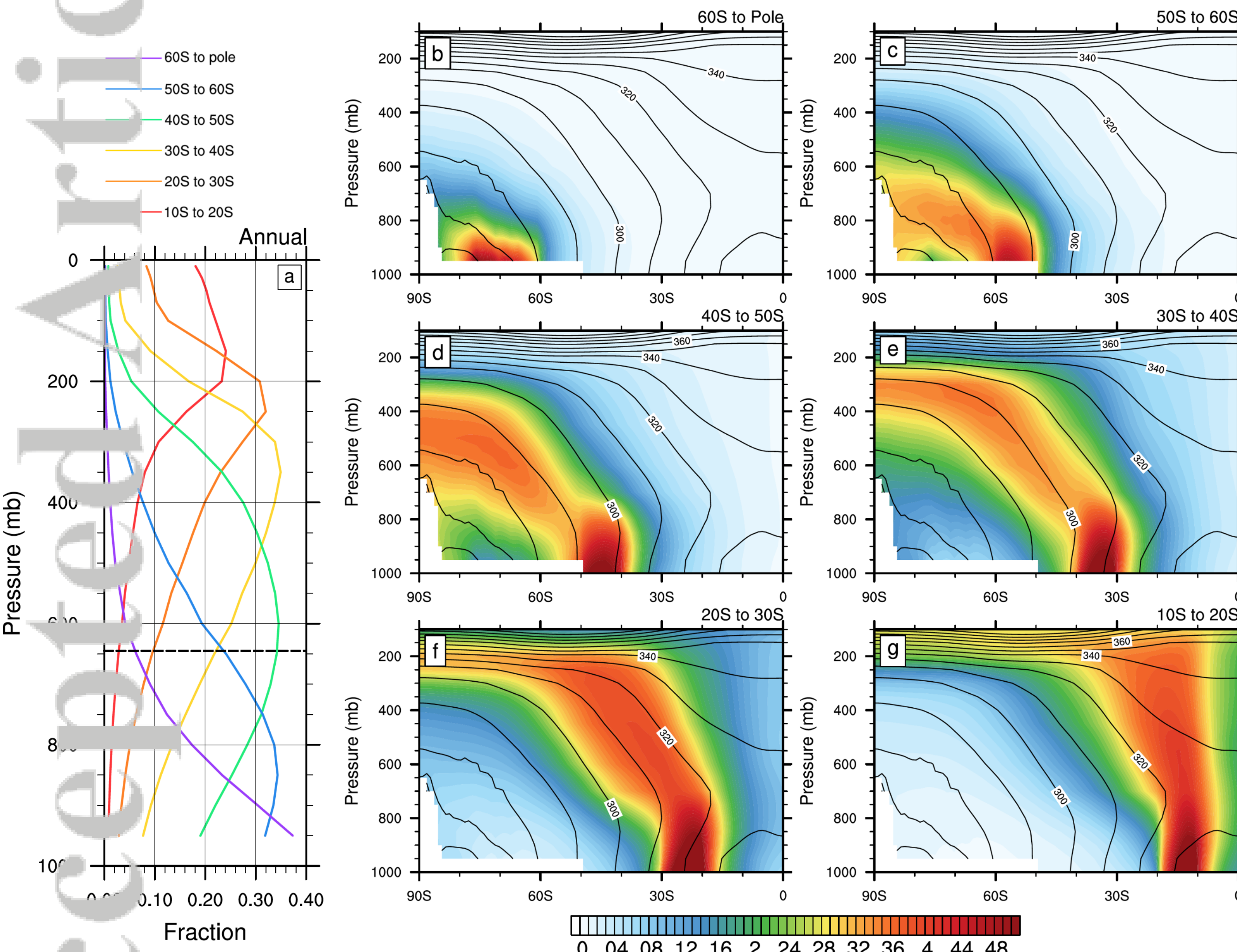
60S to pole
50S to 60S
40S to 50S
30S to 40S
20S to 30S
10S to 20S
Annual
a
Pressure (mb)
Fraction
0.10
0.20
0.30
0.40
0
200
60S to Pole
50S to 60S
40S to 50S
30S to 40S
20S to 30S
10S to 20S
b
c
d
e
f
g
Pressure (mb)
200
400
600
800
1000
90S
60S
30S
0
300
320
340
360
.0 .04 .08 .12 .16 .2 .24 .28 .32 .36 .4 .44 .48

Figure2.

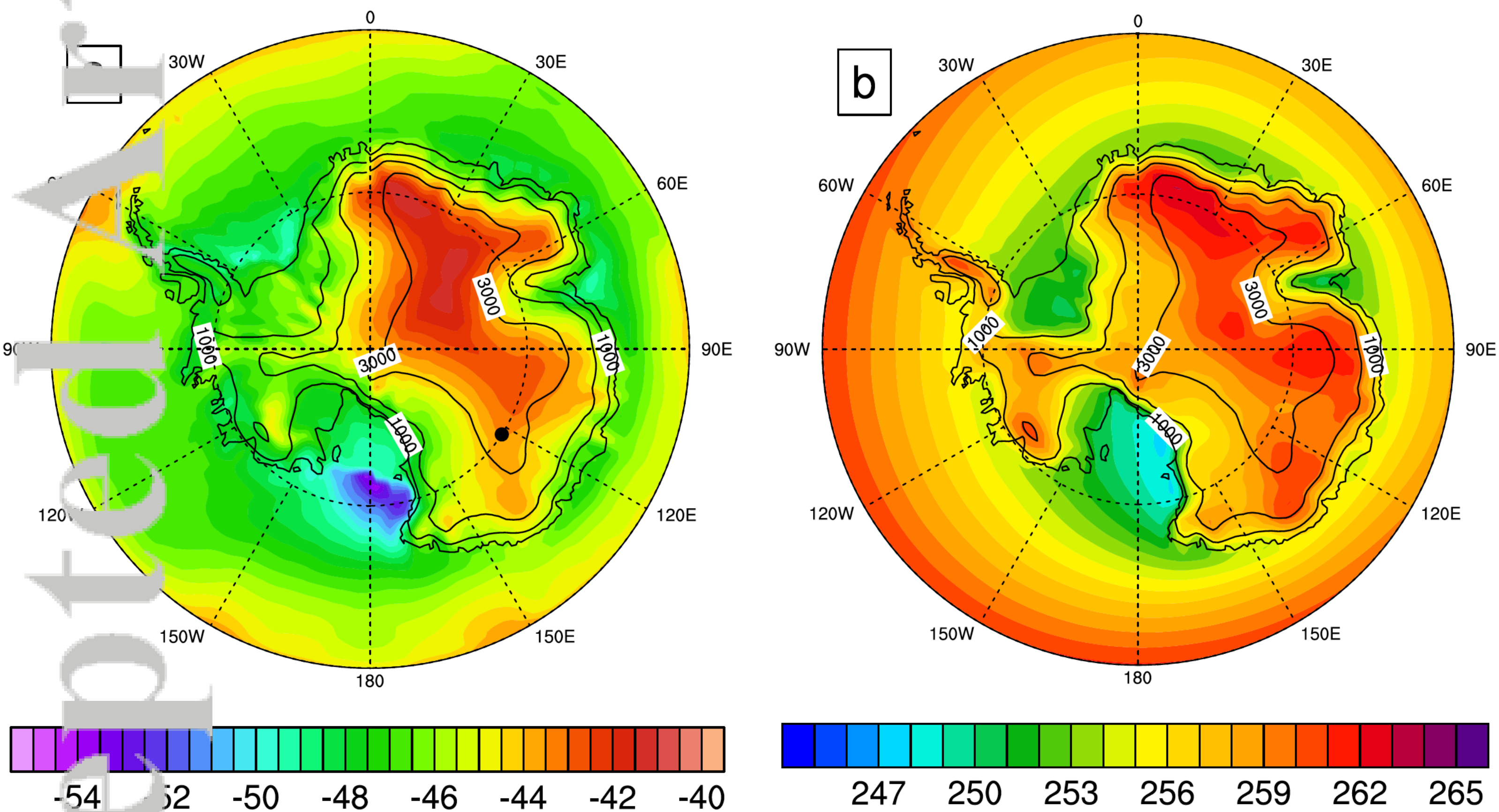

0
30W
30E
60E
90E
120E
150E
180
150W
120W
3000
1000
-54
-52
-50
-48
-46
-44
-42
-40
b
0
30W
30E
60W
60E
90W
90E
120W
120E
150W
150E
180
3000
1000
247
250
253
256
259
262
265

Figure3.

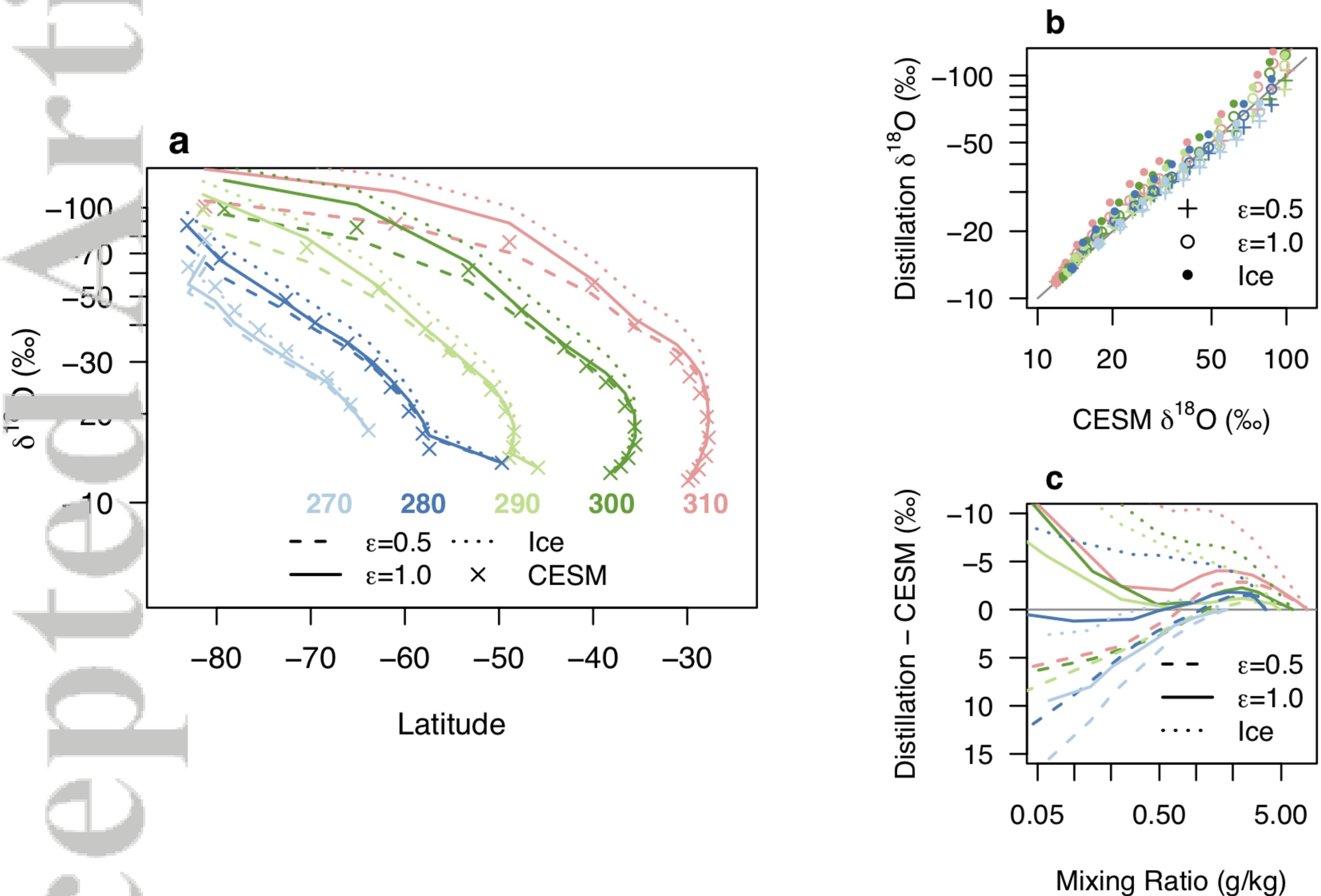
a
δ18O (‰)
−100
−70
−50
−30
−20
−10
−80
−70
−60
−50
−40
−30
Latitude
270
280
290
300
310
ε=0.5
Ice
ε=1.0
CESM
b
Distillation δ18O (‰)
CESM δ18O (‰)
−100
−50
−20
−10
10
20
50
100
ε=0.5
ε=1.0
Ice
c
Distillation − CESM (‰)
−10
−5
0
5
10
15
0.05
0.50
5.00
Mixing Ratio (g/kg)
ε=0.5
ε=1.0
Ice

Figure4.

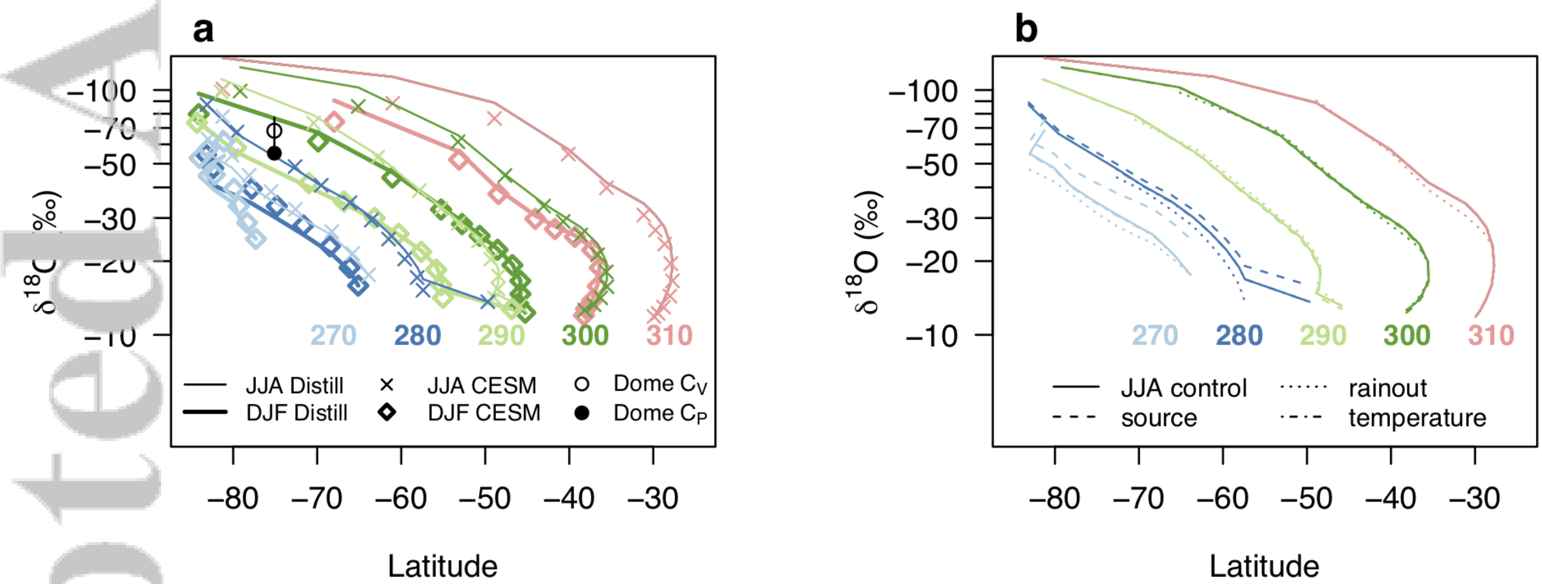
a
b
270
280
290
300
310
JJA Distill
DJF Distill
JJA CESM
DJF CESM
Dome C_V
Dome C_P
JJA control
source
rainout
temperature
$\delta^{18}O$ (‰)
Latitude
−100
−70
−50
−30
−20
−10
−80
−70
−60
−50
−40
−30

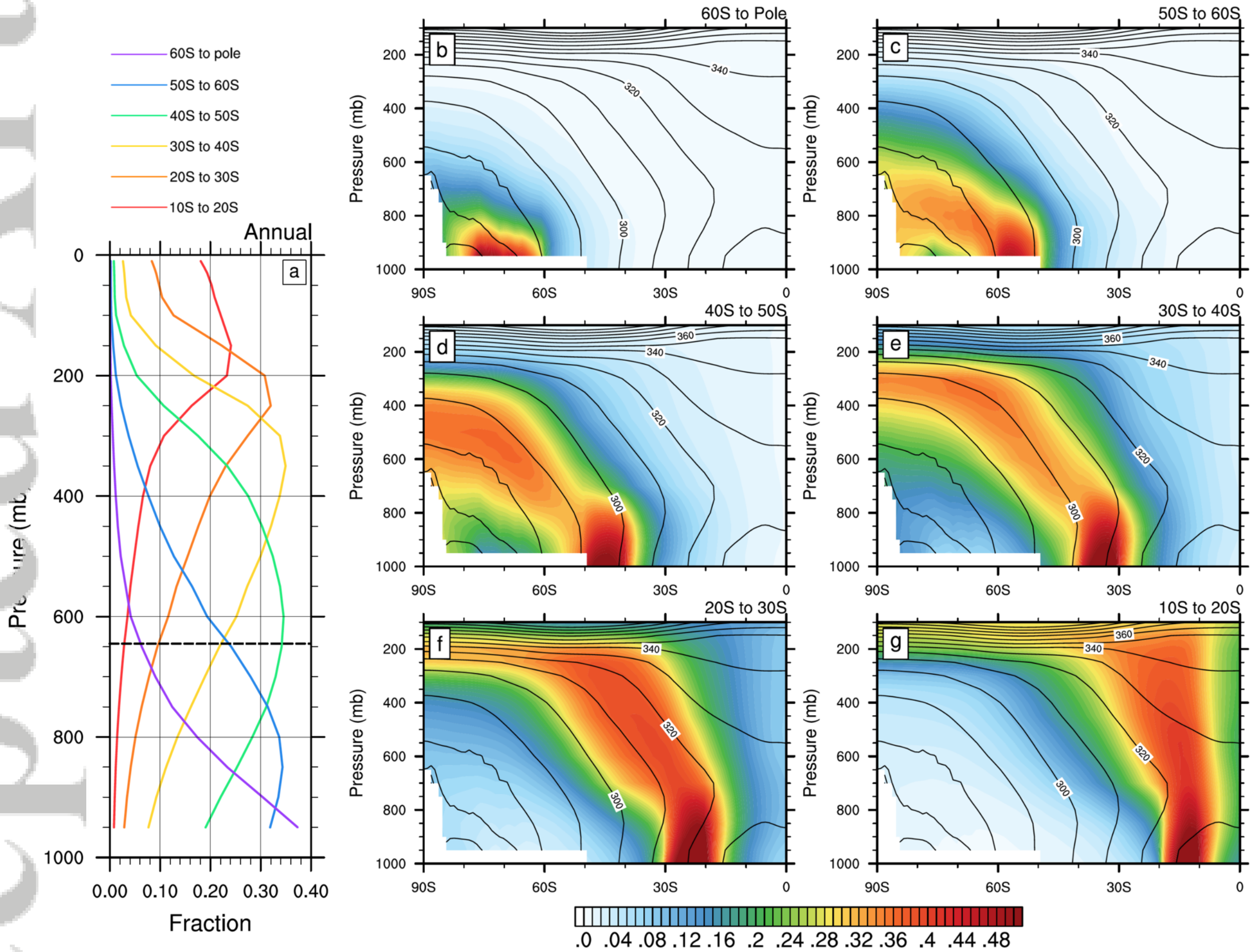

2019GL082965-f01-z-.tif

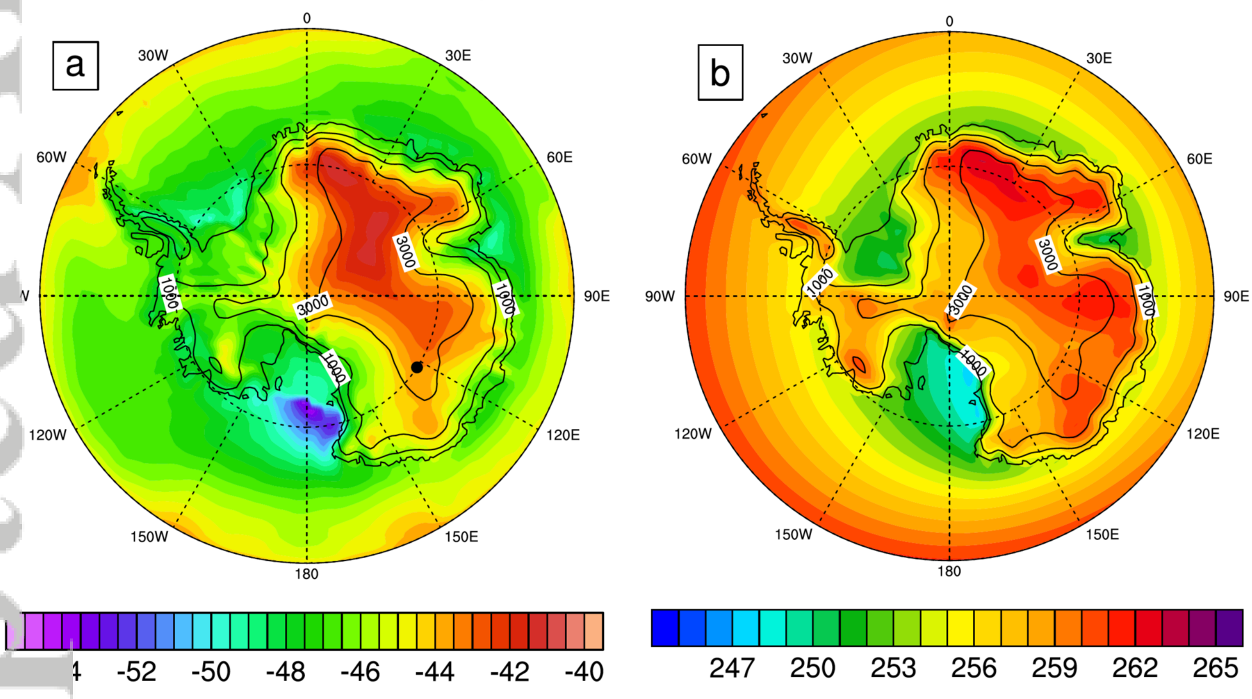

2019GL082965-f02-z-.tif

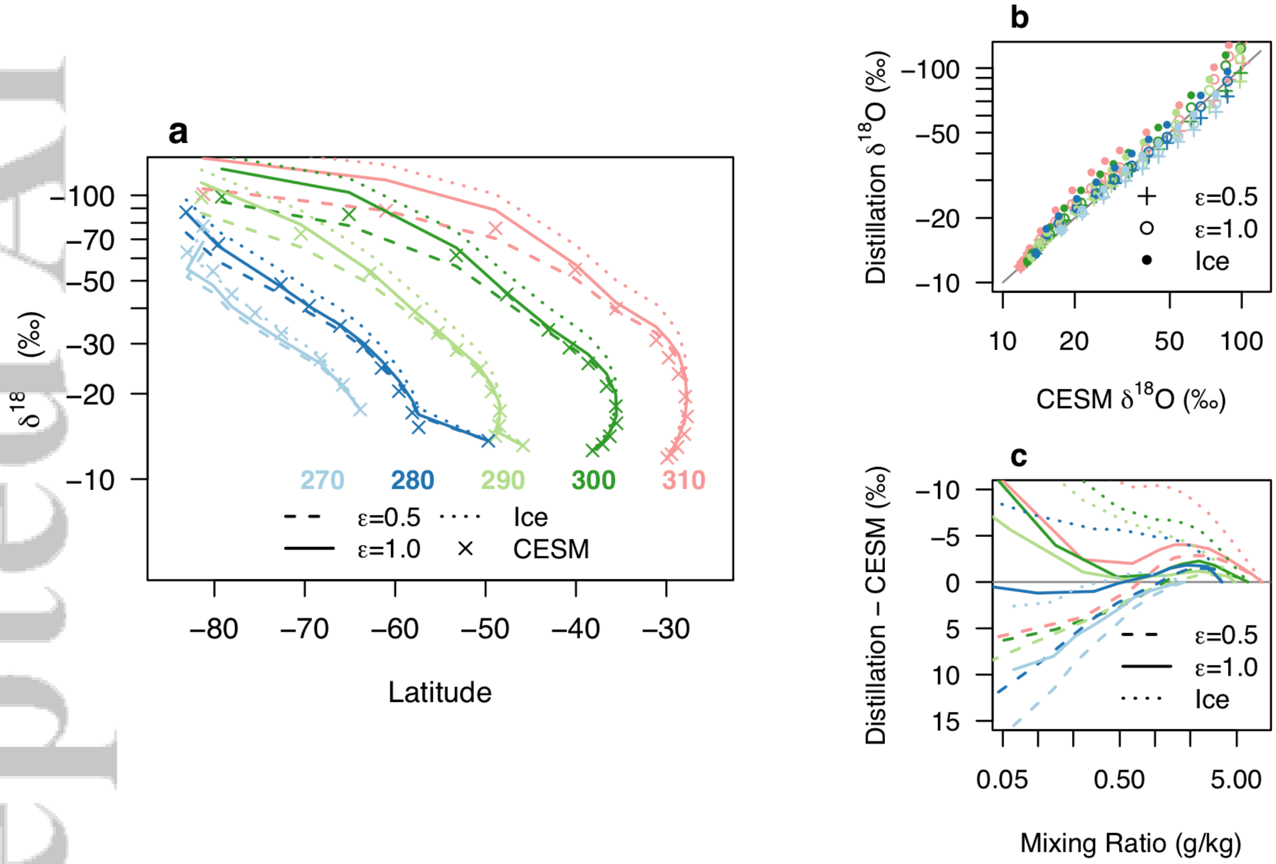

2019GL082965-f03-z-.tif

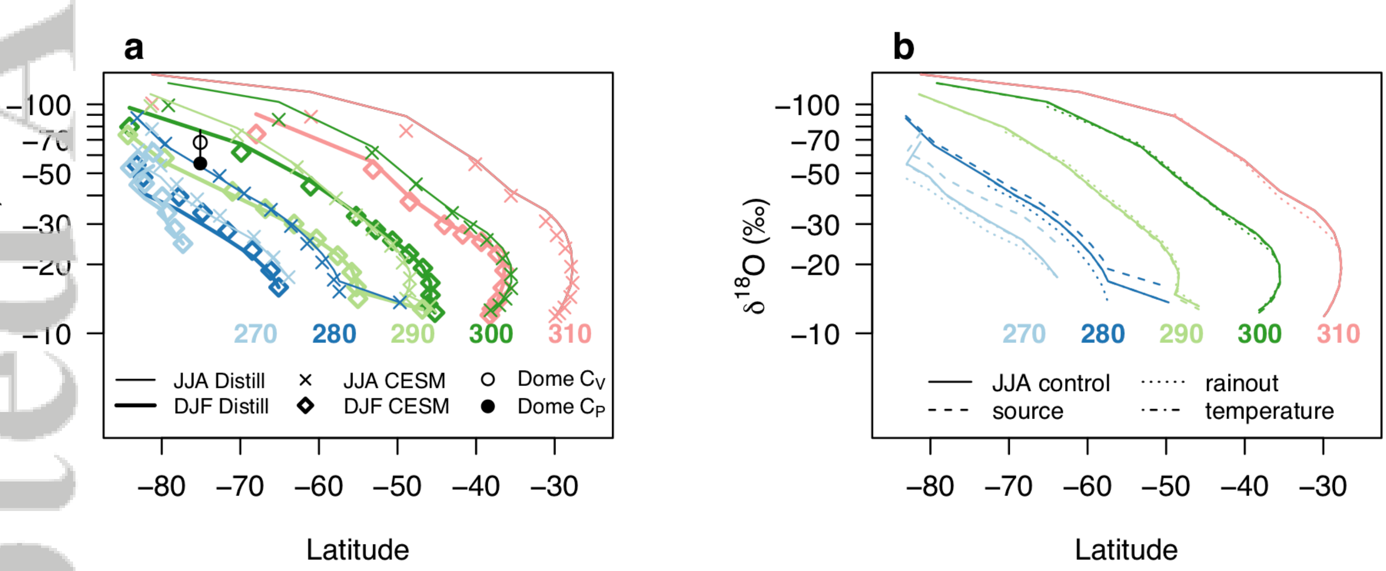

2019GL082965-f04-z-.tif